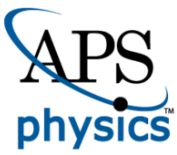

Distribution of Supercurrent Switching in Graphene under the Proximity Effect

U. C. Coskun, M. Brenner, T. Hymel, V. Vakaryuk, A. Levchenko, and A. Bezryadin

Phys. Rev. Lett. **108**, 097003 — Published 28 February 2012

DOI: 10.1103/PhysRevLett.108.097003

Distribution of supercurrent switching in graphene under proximity effect

U. C. Coskun,[1, 2, *] M. Brenner,[1] T. Hymel,[1] V. Vakaryuk,[3] A. Levchenko,[4] and A. Bezryadin[1]

[1]*Department of Physics, University of Illinois at Urbana-Champaign, Urbana, Illinois 61801, USA*
[2]*Department of Physics, University of Texas, Dallas, Texas 75080, USA*
[3]*Materials Science Division, Argonne National Laboratory, Argonne, Illinois 60439, USA*
[4]*Department of Physics and Astronomy, Michigan State University, East Lansing, Michigan 48824, USA*

(Dated: January 22, 2012)

We study the stochastic nature of switching current in hysteretic current-voltage characteristics of superconductor-graphene-superconductor (SGS) junctions. We find that the dispersion of the switching current distribution scales with temperature as $\sigma_I \propto T^{\alpha_G}$ with α_G as low as 1/3. This observation is in sharp contrast with the known Josephson junction behavior where $\sigma_I \propto T^{\alpha_J}$ with $\alpha_J = 2/3$. We propose an explanation using a generalized version of Kurkijärvi's theory for the flux stability in rf-SQUID and attribute this anomalous effect to the temperature dependence of the critical current which persists down to low temperatures.

PACS numbers: 74.45.+c, 72.80.Vp, 74.40.-n, 74.50.+r

Since the extraction of single-layer graphene [1, 2] much effort has concentrated on its study due to the promising potential in applications. The knowledge of graphene properties and expertise in making high quality devices have grown substantially [3–5]. Nevertheless, the transport in graphene subject to nonequilibrium conditions and in the proximity to a superconductor, an important ingredient in the majority of applications, is far from being fully understood. Unlike metal-superconductor interfaces reflection from a graphene-superconductor boundary is governed by the *specular* Andreev processes [6]. This peculiar effect combined with the unique band structure of graphene makes proximity effect in graphene a particularly interesting subject to study.

Recent experiments on the superconductor-graphene-superconductor (SGS) devices have revealed many interesting features caused by the proximity effect [7]. These include an observation of supercurrent and subsequent measurement of the current-phase relation, signatures of multiple Andreev reflection in the differential conductance, and Shapiro steps under microwave irradiation, see Refs. [8–12]. Recent measurements have also revealed the residual resistance of SGS junctions for currents below critical which was attributed to the phase diffusion phenomenon [13] followed by the crossover to macroscopic quantum tunneling regime at low temperatures [14]. Here we report first systematic study of thermally activated dynamics of phase slips in SGS junctions through the measurement of the switching current distribution.

Measurement of the decay statistics of metastable states is a powerful tool for revealing the intrinsic thermal and quantum fluctuations. In the Josephson junctions (JJ) a metastable dissipationless (superconducting) state decays into dissipative (phase slippage) state when the bias current I reaches a critical value called switching current I_{SW}, which is stochastic. Analysis of the distribution of the switching current was employed to reveal macroscopic quantum tunneling in JJs [15], superconducting nanowires [16], small underdamped JJs [17] and intrinsic JJs in high-T_c compounds [18]. Experimentally observed temperature dependence of the switching current dispersion σ_I always follows a power law $\sigma_I \propto T^{2/3}$, if the switching is induced by a single thermally activated phase slip [19]. However at sufficiently low temperatures the temperature dependence of σ_I saturates, which is usually attributed to the macroscopic quantum tunneling [15].

Study of switching current distribution in conventional SNS junctions, where N is normal metal, is obstructed by the fact that such junctions are usually overdamped. As a result their I-V characteristics are smooth and the notion of the switching current is not applicable. Here we report a study of moderately underdamped SGS junctions with the quality factor $Q \simeq 4$ for the entire span of gate voltages. Our main finding is the anomalous temperature dependence of the switching current dispersion $\sigma_I \propto T^{\alpha_G}$ in SGS devices with $0.3 \lesssim \alpha_G \lesssim 0.5$, which persists for a wide range of gate-induced doping and is significantly smaller than the usual $\alpha_J = 2/3$. In general, any power law different from 2/3 is associated with the possibility of quantum phase slips. In our graphene-based proximity junctions, although the power law notably deviates from 2/3, we argue that thermally activated phase slips are the major contributor. We interpret an anomalous dispersion of σ_I by using a generalized Kurkijärvi model [20]. Our conclusion is that the slowed temperature scaling of σ_I in SGS junction is due to the substantial temperature dependence of the critical current, which persists down to low temperatures in SGS systems.

Graphene flakes are deposited on 280 nm thick SiO_2 surface using mechanical exfoliation [1]. Raman spectroscopy is used to confirm the number of layers [21]. The electrodes, which have a fingered shape (Fig. 1a), are patterned from a bilayer Pd/Pb (4nm/100nm), as

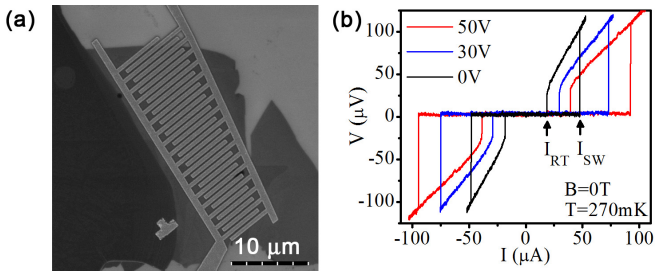

FIG. 1: [Color online] a) SEM micrograph of sample 105. Distance between the electrodes along the current (length of the junction) is $L = 265$ nm. Width of the junction (distance across the current) is $W = 214$ μm. For sample 111s, $L = 280$ nm and $W = 9.9$ μm. b) The hysteretic I-V curves of SGS junction (sample 105) taken at various gate voltages. The switching I_{SW} and retrapping I_{RT} currents are shown.

explained in the supplementary materials (SM). In order to measure the switching current distribution, the amplitude of the sinusoidal current bias is set somewhat higher than the maximum switching current, and it is adjusted when needed to keep the sweep speed roughly constant. The number of switching events for each distribution was either 5000 (for the sample 111s) or 10000 (for the sample 105). At low temperatures the I-V curves of the samples exhibit a hysteretic behavior, Fig. 1b, which enables us to study switching current statistics.

Our main focus is on the $\sigma_I(T)$ function. Figure 2 shows a switching histogram for sample 105 at (a) Dirac point ($V_g = -30V$) and (b) $V_g = 50V$. During the experiment, some anomalously premature switching events are recorded. These events, which significantly deviate from the general population of the distribution, are very rare and are believed to be unrelated to thermal fluctuations. In order to exclude these anomalous jumps from the standard deviation calculation we first convert the raw data to the switching rate $\Gamma(I)$ according to the Kurkijarvi method [19, 20]. The Kramers and Stewart-McCumber theories combined (see below) lead to the expectation that $\ln\Gamma \propto (1-I/I_C)^{3/2}$. In Figs. 2c and 2d we plot $\ln\Gamma$ versus $(1-I/I_C)^{3/2}$. The critical current I_C is tuned to make the graph as linear as possible. Then the linear part of the graph is fit with a straight line. Hollow squares and circles are the measured data. Filled symbols are those points which were used to find the best linear fits. The best fit $\Gamma(I)$ is then used to regenerate the distribution of I_{SW} by inverting the Kurkijärvi transformation. The results are shown as black curves in Fig. 2a and Fig. 2b, for the experimental sweep rates were $363\,\mu$A/s and $2.7\,$mA/s. The red curves are computed distributions for $dI/dt = 100\,\mu$A/s and $1.0\,$mA/s correspondingly. The dispersion σ_I is then computed for the same value of dI/dt for all temperatures.

Our main results are presented in Fig. 3. This figure shows standard deviation σ_I and critical current I_C versus temperature for various gate voltages. Figures 3a and 3b are log-log plots of σ_I versus T. The best linear fit provides α_G, which is defined by the equation $\sigma_I \propto T^{\alpha_G}$. The estimated error or uncertainty in the power values is about 7%. Overall, the best fit α_G's are different from the theoretically predicted JJ value $\alpha_J = 2/3 = 0.667$. Since numerous previous experiments on JJs established the power close to 2/3 while our data indicate powers roughly between 1/3 and 1/2, an understanding of such discrepancy is desirable.

We interpret these observations based on the following model. Since the pioneering theoretical work of Kurkijärvi [20] and its experimental confirmation by Fulton and Dunkleberger [19] kinetics of stochastic phase slips in the JJs is described within Stewart-McCumber model [23], which employs sinusoidal current-phase relation (CPR), $I_S(\phi) = I_C \sin(\phi)$, and represents the total current as a sum of superconducting, normal and displacement components. At the mesoscopic scale and, in particular, in the context of graphene proximity circuits, there are reasons to question the applicability of such model given the possibility of a highly nontrivial structure of $I_S(\phi)$ (see SM). This naturally raises a question about the universality of the previous results with respect to the form of the CPR. It is rather remarkable to realize that the predictions of the theory [20] in fact extend be-

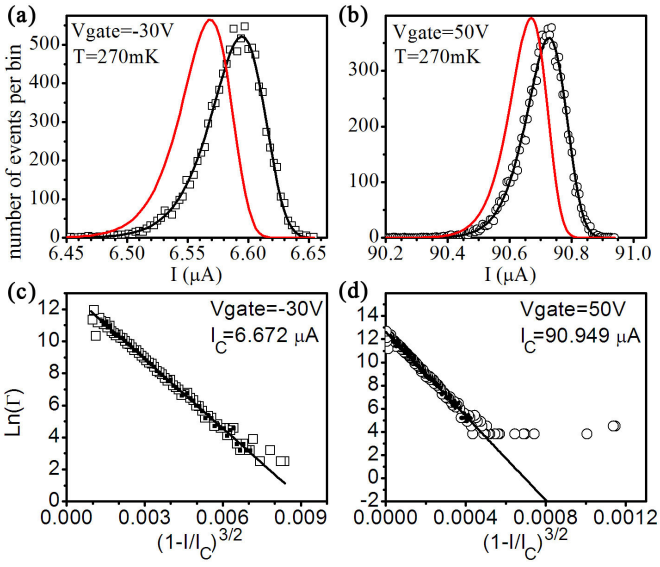

FIG. 2: [Color online] (a), (b) Switching current distributions at Dirac point ($V_g = -30\,V$) and $V_g = 50\,V$. The black curve shows a theoretical fit to the experimental distribution with an experimental speed: (a) $363\,\mu$A/sec and (b) 2.7 mA/sec. The red curve shows a calculated distribution with a new sweeping speed: (a) $100\,\mu$A/sec and (b) 1.0 mA/sec, using the escape rate to the standardized sweep speed. (c)–(d) Logarithm of the escape rate is shown as a function of the scaled current. The raw data are shown as hollow circles and squares. Filled squares and circles are used to calculate the critical current and to fit the escape rate, which is shown as a solid line. Anomalous premature jumps are visible as isolated data on the left side of the graph.

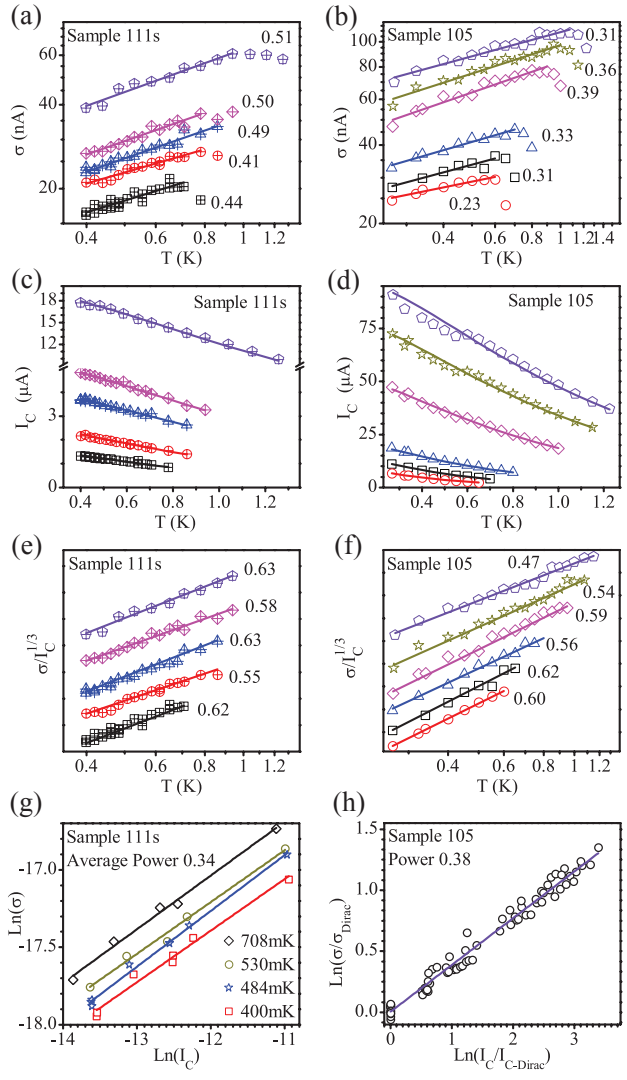

FIG. 3: [Color online] For sample 111s ($V_{gD} = -1\,\mathrm{V}$) data sets on panels (a), (c) and (e) correspond to gate voltages V_g=50, 5, 3, 1, and -1 V, from top to bottom. For sample 105 ($V_{gD} = -30\,\mathrm{V}$) data sets on panels (b), (d), (f) correspond to V_g=50, 30, 10, -10, -30, and -50 V, from top to bottom. (a)–(b) Standard deviation vs. temperature, in the log-log format. The best linear fits determine the power α_G, which is shown near each fit. (c)–(d) Critical current vs. temperature for sample 105 and 111s at various gate voltages. Solid lines are theoretical fits [25]. (e)–(f) Normalized standard deviation, $\sigma_I/I_C^{1/3} \propto T^{\tilde{\alpha}_G}$, vs. temperature, in the log-log format. The corresponding powers $\tilde{\alpha}_G$ are indicated. The graphs are shifted vertically for clarity. (g) Log-log plot of standard deviation vs. critical current at four different temperatures. (h) Log-log plot of the scaled standard deviations vs. scaled critical current.

yond the limits of its original validity. We now proceed to the generalization of the Kurkijärvi's theory [20] developed for the statistics of thermally activated phase slips in a flux-biased rf-SQUID to the case of a current-biased weak link with an *arbitrary* CPR.

Within the Stewart-McCumber model the dynamics of the phase ϕ is equivalent to the dynamics of a viscous Brownian particle subject to the following external potential:

$$G(\phi) = F(\phi) - \hbar I\phi/2e\,, \qquad (1)$$

which is the Gibbs potential. Here $F(\phi) = (\hbar/2e)\int d\phi I_S(\phi)$ is the free energy and I is the bias current. We assume that $I_S = I_S(\phi)$ is a single-valued smooth function. For $I = 0$, $G(\phi)$ is a periodic function of ϕ with alternating local maxima and minima. In the absence of fluctuations the phase is trapped in one of the minima as long as $I < I_C$, which is a state with zero voltage. In the resistive state when $I > I_C$ the phase increases with time. In the presence of thermal fluctuations even at $I < I_C$ the phase can escape its local minimum, i.e. experience a phase slip, which drives the junction into a phase-running resistive state. Such a process is detected as a voltage jump (a switching event) on the I-V curve. Upon decreasing I the junction may show hysteretic behavior and the quality factor Q determines the width of the hysteretic region. The activation rate of a phase slip for a moderately underdamped ($Q \gtrsim 1$) to overdamped ($Q \ll 1$) junction is given by Kramers theory [24] (hereafter $k_B = 1$)

$$\Gamma = (1/2\pi)\left(\sqrt{\eta^2/4 + \omega^2} - \eta/2\right)\exp(-\Delta G/T)\,. \qquad (2)$$

The energy barrier ΔG is the spacing between two consecutive extrema: $\Delta G = G(\phi_+) - G(\phi_-)$. The prefactor is determined by the curvature of the potential at minimum, $\omega^2 = C^{-1}(2e/\hbar)^2\partial_\phi^2 G$ and by the damping parameter $\eta = 1/R_N C$, where R_N and C are effective normal resistance and capacitance of the junction. Notice that $Q = \omega_p/\eta$ where $\omega_p = \sqrt{2eI_C/\hbar C}$ is plasma frequency.

To find the activation barrier $\Delta G(I)$ let us introduce a critical phase ϕ_C defined through $I_C = I_S(\phi_C)$. In the vicinity of ϕ_C one can use Taylor expansion $I_S(\phi) = I_C - \frac{1}{2}|I_C''|(\phi - \phi_C)^2$ provided $I_S(\phi)$ is a smooth function. $F(\phi)$ is obtained by integrating the supercurrent over the phase, which gives $F(\phi) = F_C + \frac{\hbar}{2e}I_C(\phi - \phi_C) - \frac{1}{3!}\frac{\hbar}{2e}|I_C''|(\phi - \phi_C)^3$, where $F_C = F(\phi_C)$ and $I_C'' = \partial_\phi^2 I(\phi)|_{\phi_C}$. These equations determine the locations of the two consecutive extrema of the Gibbs potential: $\phi_\pm - \phi_C = \pm\sqrt{2(I_C - I)/|I_C''|}$. Using Eq. (1) one finds

$$\Delta G(I) = G_C(1 - I/I_C)^{3/2}\,,\ G_C = \frac{2\sqrt{2}\hbar I_C}{3e}\sqrt{\frac{I_C}{|I_C''|}}\,. \qquad (3)$$

The curvature of the Gibbs potential at the extrema points can be obtained in a similar way and is given by $\omega^2 = \omega_p^2\sqrt{2(|I_C''|/I_C)(1 - I/I_C)}$.

The knowledge of the decay rate (Eq. 2) allows one to determine the probability p that a phase slip occurred by the time t, which reads: $p(t) = 1 - e^{-\int_0^t \Gamma(t')dt'}$, where $\Gamma = \Gamma(I(t))$. Note that the probability of not having a phase slip by the time t is $1 - p$. For a constant bias

current sweep $\omega_i = I_C^{-1} dI(t)/dt$ the probability p can be evaluated analytically. Introducing reduced current variable $u = (G_C/T)^{2/3}(1-I/I_C)$ and recalling the definition of the quality factor one obtains the following expression:

$$p = 1 - e^{-Xe^{-u^{3/2}}}, \quad X = \frac{2T\omega_p^2/(3\pi\omega_i \eta G_C)}{1+\sqrt{1+Q^2(T/G_C)^{1/3}u^{1/2}}}. \tag{4}$$

This result for the probability of a phase slip holds for a moderate to high damping provided $G_C \gg T$, the condition which is very well satisfied in most of our measurements. In the limit of high damping when $Q \to 0$ and $X \to T\omega_p^2/(3\pi\omega_i \eta G_C)$ one recovers the result of [20].

To evaluate the dispersion of the switching current we notice that the probability distribution $P(x)$ of a variable x is obtained from $p(x)$ by the differentiation with respect to x i.e. $P(x) = -dp(x)/dx$. Given the relation between the bias current I and the reduced current u this implies that the dispersions of these variables are related as $\sigma_I = I_C(T/G_C)^{2/3}\sigma_u$. The crucial observation is that dispersion σ_u considered as a function of X is constant within a few percent while X is varied by several orders of magnitude, so that for all practical purposes σ_u is temperature independent [20]. Using Eq. (3) and assuming that the temperature scalings of I_C and I_C'' are the same we obtain the following temperature scaling for the dispersion of switching current:

$$\sigma_I(T) \simeq (T/\Phi_0)^{2/3} I_C^{1/3}(T)\,, \tag{5}$$

where $\Phi_0 = h/2e$ is the flux quantum. Eq. (5) is the main result of the calculation, which describes the temperature dependence of σ_I for *any* smooth CPR. According to Eq. (5) the power of 2/3 in the temperature scaling for σ_I is only expected if $I_C(T) = const$. In the SGS junctions the critical current keeps increasing down to the very low temperatures (Fig. 3c and 3d), due to the divergence of the normal metal coherence length in graphene, thus leading to the stronger proximity effect. The solid lines in the figures are the fits to the SNS junction theory [25]. The fitting parameters for the theoretical fits are mean free path l_e=10-25 nm, which is similar to previously reported values [8–10], and the normal resistance R_N, which is of the same order of magnitude as the one measured directly.

To further confirm our conclusions we plot $\sigma_I/I_C^{1/3}$ versus the temperature as suggested by Eq. (5). The results are shown in Fig. 3e and 3f. Such critical-current-normalized dispersion obeys the power law with the power close to 0.6. For sample 105, the power rests between 0.47 and 0.62; for sample 111s these values vary between 0.55 and 0.63, which are close to 2/3, predicted by the adopted Kurkijärvi model.

Another type of scaling which is suggested by Eq. (5) and which can be accessed experimentally is the dependence of the dispersion on the critical current at *constant* temperature. Doping-dependent conductivity of graphene provides a unique possibility to vary the critical current while keeping the temperature constant - an experimental "knob" which is inaccessible for other types of junctions.

In Figs. 3g and 3h we present results of such measurements. We plot the $\ln(\sigma_I)$ versus $\ln(I_C)$ for various temperatures (Fig. 3g) and scaled $\ln(\sigma_I)$ versus scaled $\ln(I_C)$ (Fig. 3h). The average value of the power for sample 111s is 0.34. The power of scaled data for sample 105 is 0.38, which is shown as the best fit of the data. The resulting powers are very close to the theoretically expected value of 1/3.

In summary, we have studied the dispersion of the switching current distribution in moderately underdamped SGS junctions with clear hysteretic I-V characteristics. A systematic measurements of both temperature and critical current scaling (at constant T) of the dispersion is performed. The latter study, unavailable in regular junctions, is made possible by a gate-voltage-tuned conductivity of graphene. The temperature scaling of the switching dispersion shows unusual power laws, which is explained theoretically by taking into account the temperature variation of the critical current. The critical current scaling of the dispersion is explained theoretically by combined Stewart-McCumber and Kurkijärvi models, and is applicable for the mesoscopic junctions with arbitrary current-phase relationships.

The work was supported by ONR grant N000140910689. V.V. was supported by the Center for Emergent Superconductivity funded by DOE, under Award No. DE-AC0298CH1088.

* uccoskun@gmail.com

[1] K. S. Novoselov, *et al.*, Nature **438**, 197 (2005).
[2] Y. Zhang, *et al.*, Nature **438**, 201 (2005).
[3] A. K. Geim and K. S. Novoselov, Nat. Mater. **6**, 183 (2007).
[4] A. K. Geim, Science **324**, 1530 (2009).
[5] A. H. Castro Neto, *et al.*, Rev. Mod. Phys. **81**, 109 (2009).
[6] C. W. J. Beenakker, Phys. Rev. Lett. **97**, 067007 (2006); Rev. Mod. Phys. **80**, 1337 (2008).
[7] H. Meissner, Phys. Rev. Lett. **2**, 458 (1959).
[8] H. B. Heersche, *et al.*, Nature **446**, 56 (2007).
[9] F. Miao, *et al.*, Science **317**, 1530 (2007).
[10] X. Du, I. Skachko, and E. Y. Andrei, Phys. Rev. B **77**, 184507 (2008).
[11] C. M. Ojeda-Aristizabal, *et al.*, Phys. Rev. B **79**, 165436 (2009).
[12] D. Jeong, *et al.*, Phys. Rev. B **83**, 094503 (2011).
[13] I. V. Borzenets, *et al.*, Phys. Rev. Lett. **107**, 137005 (2011).
[14] G. H. Lee, *et al.*, Phys. Rev. Lett. **107**, 146605 (2011) .
[15] J. M. Martinis, M. H. Devoret, and J. Clarke, Phys. Rev. B **35**, 4682 (1987).
[16] M. Sahu, *et al.*, Nature Physics **5**, 503 (2009); P. Li, *et al.*, Phys. Rev. Lett. **107**, 137004 (2011).

[17] H. F. Yu, *et al.*, Phys. Rev. Lett. **107**, 067004 (2011).
[18] P.A. Warburton, *et al.*, Phys. Rev. Lett. **103**, 217002 (2009).
[19] T. A. Fulton and L. N. Dunkleberger, Phys. Rev. B **9**, 4760 (1974).
[20] J. Kurkijärvi, Phys. Rev. B **6**, 832 (1972).
[21] D. Graf *et al.*, Nano Letters **7**, 238 (2007).
[22] M. Tinkahm, *Introduction to Superconductivity*, 2d ed. (McGraw-Hill Inc. 1996).
[23] W. C. Stewart, Appl. Phys. Lett. **12**, 277 (1968); D. E. McCumber, J. Appl. Phys. **39**, 3133 (1968).
[24] H.A. Kramers, Physica **7**, 284 (1940).
[25] A. D. Zaikin and G. F. Zharkov, Sov. J. Low. Temp. Phys. **7(3)**, 184 (1981); P. Dubos *et al.*, Phys. Rev. B **63**, 064502 (2001); A. Levchenko, A. Kamenev, and L. Glazman, Phys. Rev. B **74**, 212509 (2006).